Jour. of the KGS, Vol. 24, No. 9. September 2008, pp. 41~48 Technical Note

A Graphical Method for Evaluation of Stages in Shrinkage Cracking Using S-shape Curve Model

S형 곡선 모델을 적용한 수축 균열 단계 평가

Min, Tuk-Ki[1] 민 덕 기

Vo Dai Nhat[2] 보 다이 낫

요 지

본 연구에서는 수축균열 단계를 나타낼 수 있는 도해적인 방법을 제안하였다. 우선 발생된 균열들을 균열폭의 크기 순서대로 나열하여 균열 분포를 구하였다. 다음에 균열폭을 정규화하여 0에서 1사이의 값으로 나타내었다. 마지막으로 Brooks와 Corey(1964), Fredlund와 Xing(1994), van Genuchten(1980)이 제안한바 있는 S형 곡선 모델에 실험 결과를 적용시켰다. 분석 결과 van Genuchten의 식이 Brooks와 Corey식보다 정확도가 크게 높은 것으로 나타났으며, Fredlund와 Xing식보다도 높게 나타나 van Genuchten의 식을 적용하였다. 결과적으로 수축균열의 단계는 정규화된 균열폭 분포가 3개의 직선부로 나누이는 도해적인 방법으로 나타낼 수 있었다. 제안된 방법의 적용성을 보기 위해 시료의 두께에 변화를 주며 시험을 실시하였다. 측정된 데이터를 제안된 모델에 적용하여 본 결과 높은 상관성을 보여 주었다. 따라서 수축 균열은 초기수축단계, 이차수축단계 그리고 잔류수축단계의 3단계로 모사할 수 있었다. 또한 각 단계에서의 균열 폭의 범위를 제시하였다.

Abstract

The aim of this study is to present a graphical method in order to evaluate stages in shrinkage cracking. Firstly, the distribution of crack openings is established by sorting the openings of individual cracks in the soil cracking system. Secondly, it is normalized in a range of 0 to 1 to obtain the normalized crack opening distribution. Thirdly, three S-shape curve models introduced by Brooks and Corey (1964), Fredlund and Xing (1994) and van Genuchten (1980) are chosen to fit the normalized crack opening distribution using a curve fitting method. The accuracy of fitting which is described through fitting parameters by the van Genuchten equation is much higher than that by the Brooks and Corey equation and slightly higher than that by the Fredlund and Xing equation; thus the van Genuchten model is used. Finally, the stages of shrinkage cracking are graphically evaluated by drawing three separate straight lines corresponding to three linear parts of the fitted normalized crack opening distribution. The proposed method is tested with different sample thicknesses. The measured data are fitted by the selected model with the fairly high regression coefficient and small root mean square error. The results show graphically that shrinkage cracking comprises three stages; namely, primary, secondary and residual stages. Subsequently, the ranges of evaluated crack opening for each of these stages are presented.

Keywords : Curve fitting method, Fitting parameters, Graphical method, Normalized crack opening distribution, Shrinkage cracking stages, S-shape curve

1 Member, Prof. Dept. of Civil & Environ. Engrg., Univ. of Ulsan., tkmin@ulsan.ac.kr, Corresponding Author

2 Researcher, Dept. of Civil & Environ. Engrg., Univ. of Ulsan

1. Introduction

Soil cracking has been the subject of investigation for many years since it is a natural phenomenon and frequently observed in many natural and man-made structures such as buildings, dams, etc. Analysis methods for soil cracking during drying have been introduced and developed based on (i) elasticity theory, (ii) transition between tensile and shear failure, and (iii) linear elastic fracture mechanics (Morris et al., 1993). A numerical and phenomenological study has been based on the linear hygro-elasticity (Hu et al., 2006). Several theoretical problems and challenges have been summarized and introduced by Fredlund (2006). Subsequently, many researchers have attempted to study the criteria of shrinkage cracking (Horgan and Young, 2000; Kodikara et al., 2000; Konrad and Ayad, 1997; Lecocq and Vandewalle, 2003; Mal et al., 2005; Min and Vo-Dai, 2007; Peng et al., 2006; Tay et al., 2001; Velde, 1999; Velde, 2001; Vogel et al., 2005; Wijeyesekera and Papadopoulou, 2001; Yesiller et al., 2000). As water evaporates from the soil surface, the tensile stress develops in the soil system. The soil tends to crack when the tensile stress exceeds the tensile strength. They reported that cracking of clay generally depends on experiment conditions such as base material, soil density, the desiccation rate, and thickness of the sample. Conditions that govern the characteristics of soil cracking may be categorized as two separate terms: extrinsic and intrinsic conditions (Wijeyesekera and Papadopoulou, 2001). Extrinsic conditions include fundamentally the temperature, relative humidity, and wind velocity whereas moisture condition, structure of material, degree of packing, physical and chemical composition, etc. belong to intrinsic conditions.

Furthermore, soil cracking also influenced soil structure and behavior (Kodikara et al., 1999); volumetric shrinkage strain, compaction water content and hydraulic conductivity (Albrecht and Benson, 2001); and water infiltration (Liu et al., 2004). The results showed that cracking led to a considerable increase of hydraulic conductivity.

However, the development of soil cracking has been known as a complex process consisting of several stages. Thus it is important to understand the behavior of soil in the cracking process characterized by how many stages it includes. There are many different ways to describe evaluation of stages in soil cracking. In this study, we propose a graphical method to evaluate the stages of shrinkage cracking for Kaolinite clay using a S-shape curve equation based on the normalized distribution of crack opening. The proposed method is examined with several sample thicknesses. The results obtained by the proposed method provide the ranges of crack opening values for each of stages in the shrinkage cracking process.

2. Fundamentals of Shrinkage Cracking

Evaporation appears from the soil surface. Consequently, the mass of the soil for motion will be decreased by a loss of water as drying continues. The evaporation rate is affected by conditions such as temperature, relative humidity, and wind velocity and so on. The flux of soil water upward to the soil surface is mainly controlled by the hydraulic properties of the soil such as unsaturated hydraulic conductivity, water potential gradient, and thermal gradient in soil. The evaporation rate computed from the water loss is determined by both the external conditions and the internal properties of the soil system.

Shrinkage cracking is one of the most common types of cracking found in the earth structures. As water is lost from the soil surface, tensile forces are established in the drying surface layer and soil also loses its ability to relieve these tensile forces. These stresses are finally relieved by the occurrence of cracks that grow up at the surface of the soil. As the drying process develops continuously, cracks are formed successively. An individual crack propagates until it contacts with the other cracks or the borders of the container. Consequently, a network of cracks is established.

3. Graphical Method

3.1 Establishment of Crack Opening Distribution

In a network of cracks, for simplicity, a crack is defined

by a set of pixels limited by two ends (diamond symbols) as illustrated in Fig. 1 for a sample thickness of 0.01 m as an example. The openings of individual cracks are automatically calculated by applying a program written in Matlab.

Due to the occurrence of cracks, the shrinkage potential in the soil system will be reduced. Consequently, we assume that this leads to a decrease of crack opening with an increase of drying time. That means the later crack will give smaller opening than the previous one. The assumptions are appropriately verified with the results of crack opening reported by Lecocq and Vandewalle (2003) and Mal et al. (2005). Therefore, the values of crack openings (presented in Fig. 1) are sorted as shown in Fig. 2 by a dot line. In this figure, the abscissa is crack opening and the ordinate is number of crack.

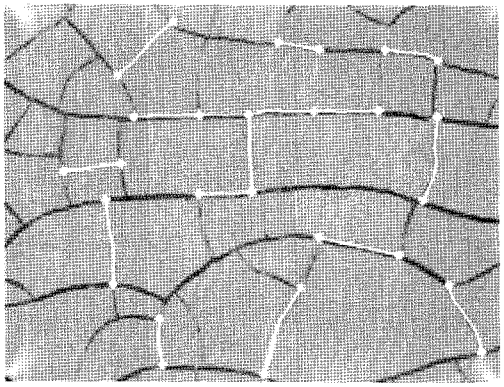

Fig. 1. Illustration of the individual cracks limited by two-diamond ends in case of 0.01 m in thickness as an example

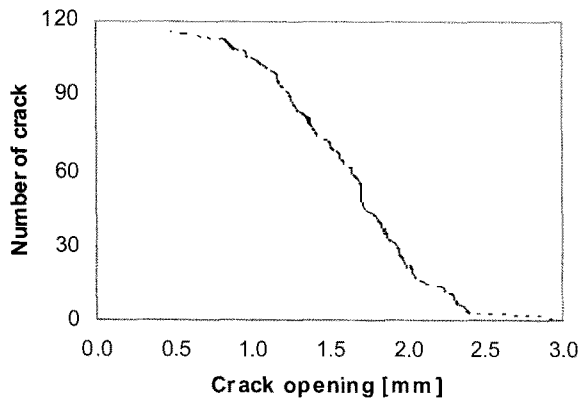

Fig. 2. The distribution of crack opening for individual cracks presented in Figure 1

3.2 Normalization of Crack Opening Distribution

Recently, S-shape curve models have been used widely to describe the relationships between soil parameters such as soil suction and volumetric water content, degree of saturation and hydraulic conductivity (Jian and Jian-lin, 2005; Kamiya et al., 2006; Sharma et al., 2002; Sharma and Mohamed, 2003; Sillers and Fredlund, 2002; Sriboonlue et al., 2006; Zhang and Chen, 2005). Each models is characterized by its parameters determined by experiment.

The crack opening distribution is normalized in a range of 0 to 1 as shown in Fig. 3 by dot line. The equations for normalizing are given as follows:

$$N_{normalized} = \frac{N - N_{\min}}{N_{\max} - N_{\min}}$$
$$W_{normalized} = \frac{W - W_{\min}}{W_{\max} - W_{\min}} \quad (1)$$

where $W_{\min}$ and $W_{\max}$ are minimum and maximum crack openings corresponding to the minimum and maximum number of crack $N_{\min}$ and $N_{\max}$, respectively. W is the measured opening corresponding to the number of crack, N.

3.3 Comparison of Three S-shape Curve Models

Based on the normalized distribution of crack opening given in Fig. 3, three S-shape curve models are used and compared to select the best model to fit the measured data. They are given as follows:

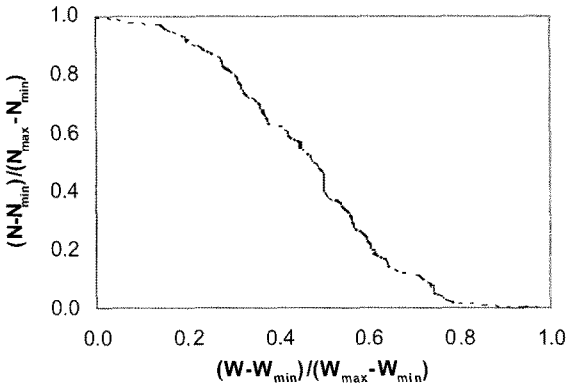

Fig. 3. The normalized distribution of crack opening obtained from Figure 2

Brooks and Corey (1964) $y = a - bx^m$ (2)

Fredlund and Xing (1994) $$y = \frac{1}{\left(\ln\left(e + \left(\frac{x}{a}\right)^n\right)\right)^m} \quad (3)$$

van Genuchten (1980) $$y = \frac{1}{\left(1 + (ax)^n\right)^m} \quad (4)$$

where a, b, n, and m are fitting parameters determined through the curve fitting method.

These models are used to fit the measured data by using the curve fitting method. The results are illustrated in Fig. 4. The normalized experiment data are denoted by dot points (by the dash dot line for the Brooks and Corey model, the dash line for the Fredlund and Xing model, and the solid line for the van Genuchten model). The Brooks and Corey model show worse fitting than the others. The fitting parameters infer that van Genuchten model is the best one consisting of the lowest values of the sum of squares due to error (SSE, i.e. 0.0484) and root mean squared error (RMSE, i.e. 0.0207), and the highest value of R-square (i.e. 0.9950). They are summarized in Table 1. Therefore, van Genuchten model is selected for fitting the experiment data in this study.

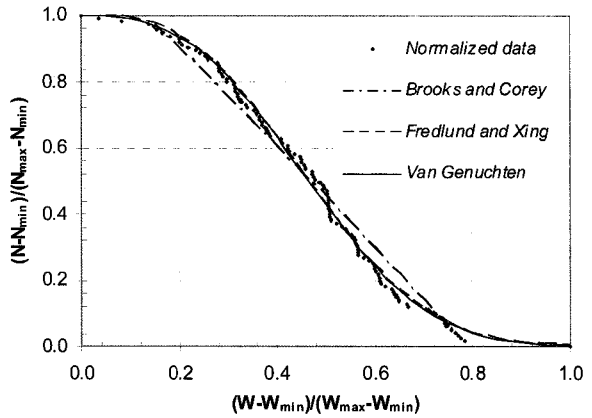

Fig. 4. The normalized distribution of crack opening (dot points) fitted by three S-shape curve models of Brooks and Corey (dash dot), Fredlund and Xing (dash line), and van Genuchten (solid line)

Table 1. Fitting parameters for three S-shape curve models

Fitting parameter	Model		
	Brooks and Corey	Fredlund and Xing	van Genuchten
SSE	0.4307	0.0543	0.0484
R-square	0.9554	0.9944	0.9950
RMSE	0.0617	0.0219	0.0207

3.4 Evaluation of Shrinkage Cracking Stages

According to the S-shape normalized distribution of crack opening fitted by the van Genuchten model in Fig. 4 (solid line), we propose a graphical method for estimating the stages in shrinkage cracking. The method is presented in Fig. 5. Three regions from the S-shape curve (solid line) are outlined separately by drawing three straight components (dot lines). The first component is determined by drawing a line tangent to the top curve through the maximum value on the ordinate; the second one is constituted by drawing a line tangent to the curve through the point of maximum slope; and the third one is a line tangent to the bottom part of the S-shape curve through the minimum value on the ordinate. The first and third straight components intersect the second one at two separate points. These two transition points evaluate the stages of cracking process described by the S-shape equation. Three shrinkage cracking stages are illustrated in Fig. 5. They are outlined by dash dot lines: namely, primary, secondary and residual stages.

From these stages of shrinkage cracking, the corresponding ranges of crack opening can be estimated by projecting two transition points to the abscissa drawn by

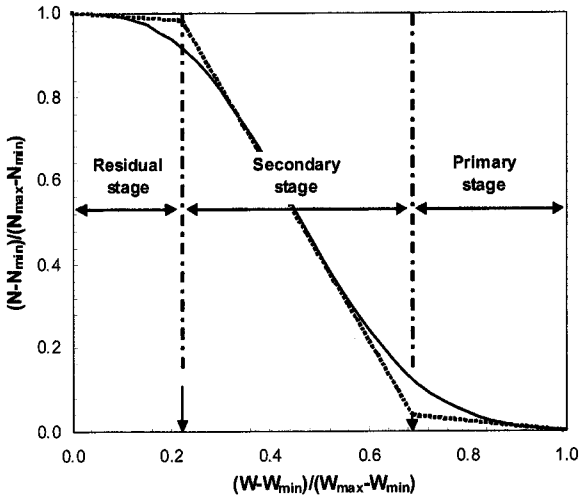

Fig. 5. Graphical method for evaluation of shrinkage cracking stages by drawing three straight components corresponding to three linear parts of the normalized crack opening distribution fitted by van Genuchten equation

the arrows as shown in Fig. 5.

4. Soil Material Properties

For the laboratory measurements, Kaolinite clay is used. The properties of Kaolinite are as follows: liquid limit, $LL = 42.07\%$; plastic limit, $PL = 25.40\%$; plasticity index, $PI = 16.67\%$; specific gravity, $G_s = 2.646$; coefficient of uniformity, $C_u = 40.75$; and coefficient of curvature, $C_c = 2.33$.

The experiments were performed in a rectangular steel tray. Firstly, the soil was carefully mixed with water and stirred for half an hour to make a paste. An initial water content of the mixture was about 65%, 1.5 times higher than the liquid limit. Secondly, the mixture was poured in the tray and uniformly spread to make the surface flat. We vary the thickness of sample with 0.005, 0.006, 0.007, 0.008, 0.009, 0.01, 0.015 and 0.02 m. Finally, the specimen was balanced and allowed to dry naturally in laboratory at room conditions. The drying process continued for several days. When cracking processing finished completely, images of the specimens were captured by a digital camera. Image analysis with an application of the control point selection technique is used to analyze the images. The proper region of image is selected to compute the opening of cracks by using a numerical program written in Matlab.

5. Experimental Results

5.1 Shrinkage Cracking Stages Evaluated by the Graphical Method

Fig. 6 presents the images of eight sample thicknesses tested. Applying the proposed method for these images resulted in the crack opening distributions as shown in Fig. 7. The experiment data are plotted by dot lines; the normalized values are denoted by dash dot lines; and continuous lines present the fitted values corresponding to the normalized ones. The resulted fitting parameters are summarized in Table 2.

As seen in Table 2, for all the cases of sample thickness, the regression coefficients are extremely high, more than 0.99; except in the case of 0.02 m (only 0.9724). Correspondingly, the values of RMSE are really small, that is, less than 5% including the case of 0.02 m thick sample. This concludes that the proposed model is properly adopted for describing the distribution of crack opening.

As shown in Fig. 7, the distributions of measured crack opening represent proximately S-shape curves with the fairly high regression coefficients as well as low RMSEs shown in Table 2. By applying the graphical method presented in this paper to each of the crack opening distributions, the ranges of shrinkage cracking stages - namely primary, secondary and residual - are tabulated in Table 3 for both the normalized and real ranges of crack opening.

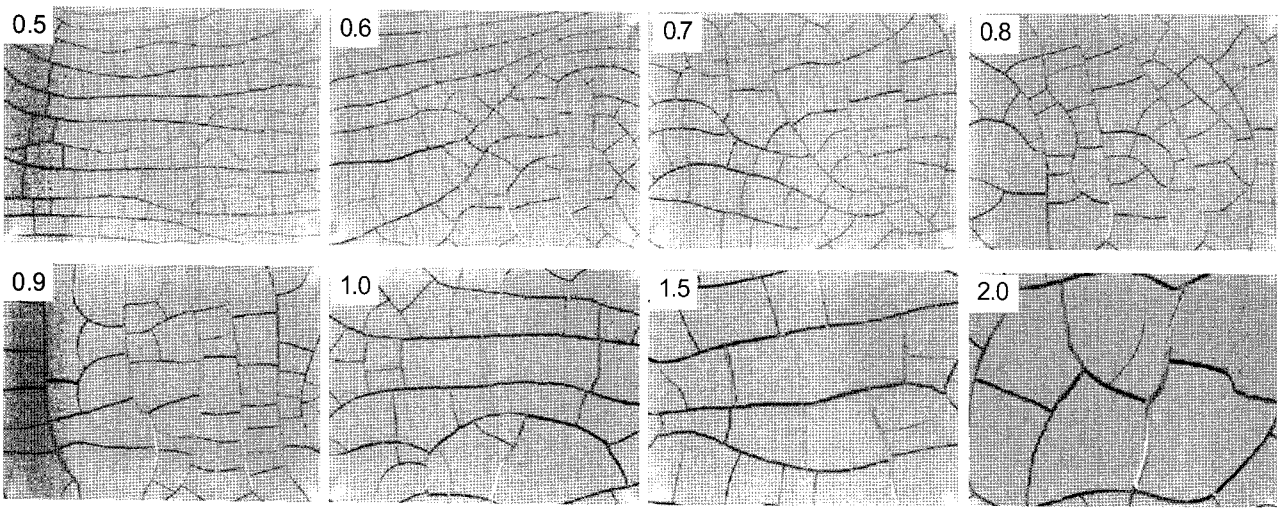

Fig. 6. Images of soil cracking with different sample thicknesses (cm)

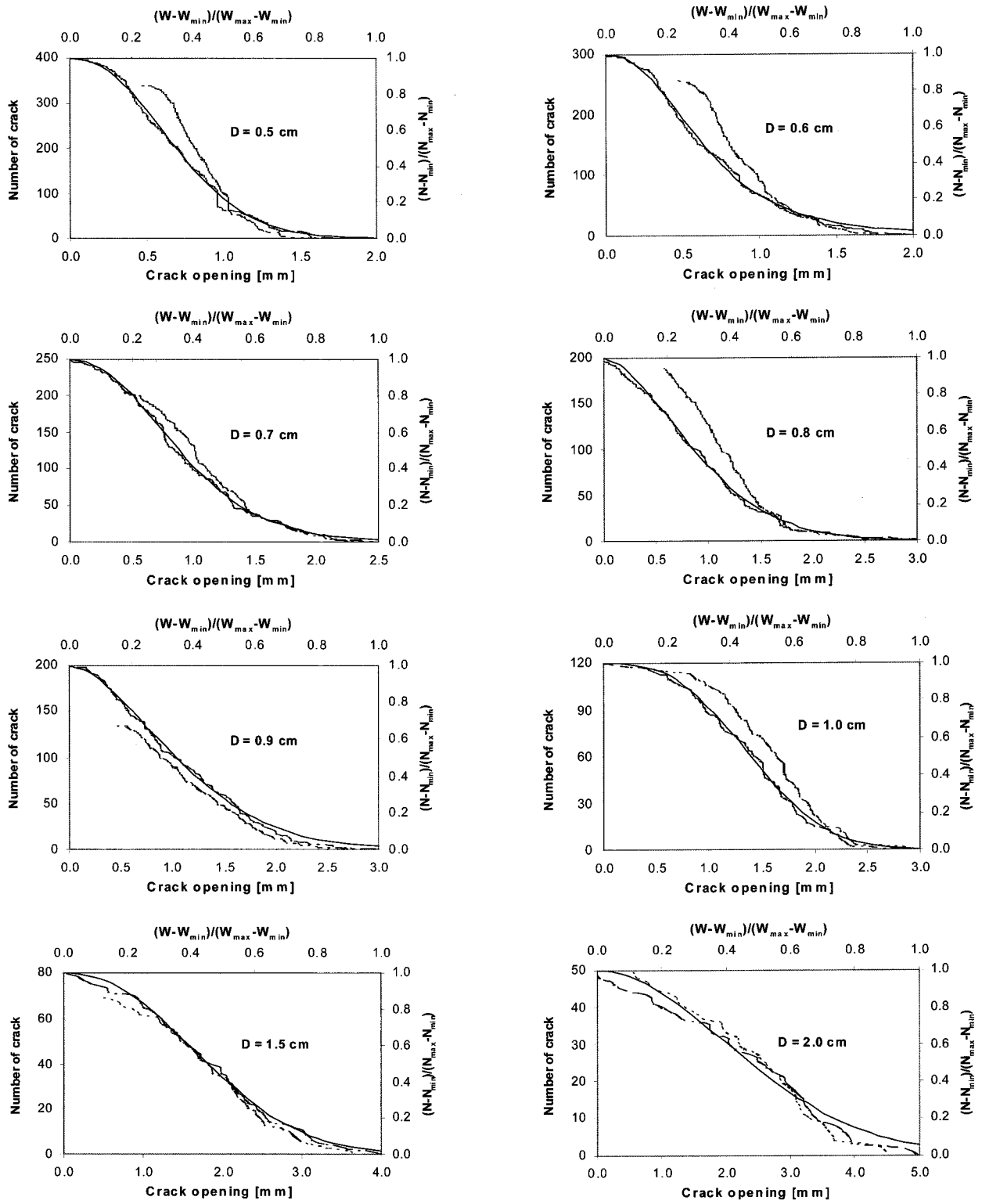

Fig. 7. Crack opening distributions for several different sample thicknesses: the dot lines are experiment data, the dash dot lines are normalized values, and the continuous lines are the evaluated values using the van Genuchten S-shape equation based on the normalized values

5.2 Additional Considerations

As reported by Kodikara et al. (2000), the measurements of soil cracking depend on the sample thickness. An observation of images with different sample thicknesses as shown in Fig. 6 indicates that the number of cracks and that of crack opening are dependent on the sample thickness. In detail, the variations of crack opening with

Table 2. Fitting parameters in the cases of sample thickness

Fitting parameter	Thickness (cm)							
	0.5	0.6	0.7	0.8	0.9	1.0	1.5	2.0
a	0.7071	2.03	1.059	0.0646	0.0729	0.2224	0.1399	0.054
m	15.63	2.12	5.726	545.7	338.5	402.1	310.1	861.9
n	2.195	2.188	2.093	1.67	1.679	2.803	2.214	1.944
R-square	0.9951	0.9949	0.9975	0.9966	0.9963	0.9950	0.9955	0.9724
RMSE	0.0203	0.0207	0.0144	0.0171	0.0177	0.0207	0.0198	0.0494

Table 3. Ranges of crack opening for shrinkage cracking stages in the cases of sample thickness (cm)

Cracking stage		Thickness (cm)							
		0.5	0.6	0.7	0.8	0.9	1.0	1.5	2.0
Primary	Normalized	0.58~1.00	0.52~1.00	0.58~1.00	0.50~1.00	0.61~1.00	0.68~1.00	0.67~1.00	0.70~1.00
	Crack opening [mm]	1.15~1.63	1.14~1.78	1.55~2.36	1.60~2.62	1.85~2.75	2.15~2.94	2.61~3.64	3.32~4.49
Secondary	Normalized	0.10~0.58	0.08~0.52	0.11~0.58	0.08~0.50	0.07~0.61	0.23~0.68	0.18~0.67	0.16~0.70
	Crack opening [mm]	0.59~1.15	0.56~1.14	0.65~1.55	0.74~1.60	0.60~1.85	1.04~2.15	1.08~2.61	1.21~3.32
Residual	Normalized	0.00~0.10	0.00~0.08	0.00~0.11	0.00~0.08	0.00~0.07	0.00~0.23	0.00~0.18	0.00~0.16
	Crack opening [mm]	0.47~0.59	0.46~0.56	0.44~0.65	0.58~0.74	0.43~0.60	0.48~1.04	0.52~1.08	0.58~1.21

sample thickness for the cases of maximum and minimum crack openings are shown in Fig. 8.

In case of the maximum, crack opening varies increasingly with an increase of sample thickness. That is because of higher shrinkage potential of larger thickness sample. This variation of crack opening can be described proximately by power law as presented in Fig. 8 with solid line.

It is verified that as cracks appear, the shrinkage potential of the soil system decreases. Hence, the opening of the generated cracks is smaller than that of the previous cracks. Particularly, the minimum crack openings in the cases of sample thickness appear to be the same as shown in Fig. 8. It can be explained that the minimum values of crack openings are obtained as the shrinkage potential of the soil system reaches to zero. Therefore, the minimum crack openings appeared to be independent of the sample thickness. Consequently, the minimum crack openings become much smaller than the maximum crack openings as the sample thickness increases as given in Fig. 8.

Similarly, it is expected that there is a fitted relationship between the number of crack and sample thickness as thickness increases. The result is given in Fig. 9 by power law with the fairly high regression coefficient, more than 0.99. However, the number of cracks decreases drastically from 0.005 to 0.01 m in thickness but it decreases slowly from 0.01 to 0.01 m in thickness. This implies that with enough relative thin samples, the number of cracks decreases considerably compared with the relative thicker samples.

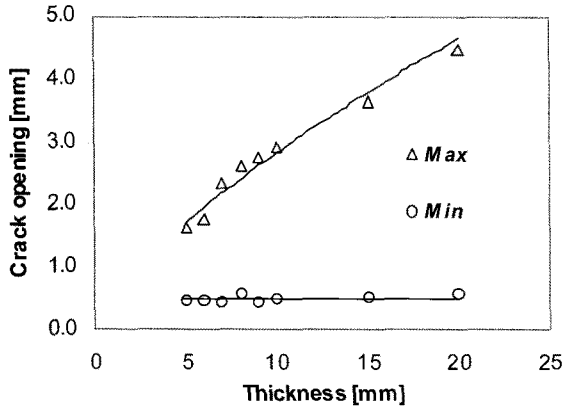

Fig. 8. The variations of crack opening with sample thickness in the cases of max and min values

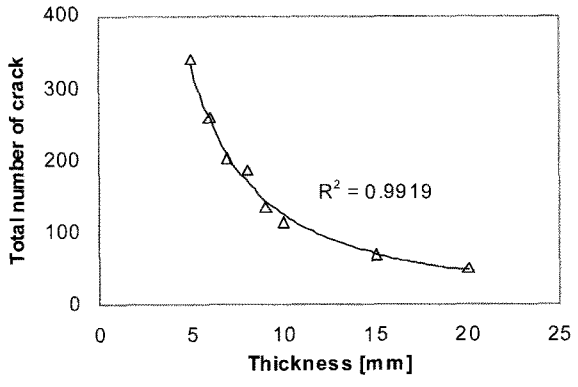

Fig. 9. The variation of total number of crack with sample thickness

6. Summary

A graphical method for evaluation of shrinkage cracking stages based on the normalized crack opening distribution represented as S-shape curve is presented. The experimental data tested with different sample thicknesses are fitted by van Genuchten model, which shows good correlation with the fairly high regression coefficient and low RMSE. Three stages in shrinkage cracking - primary, secondary and residual stages - are evaluated graphically by drawing three separately straight lines corresponding to three linear parts of the fitted normalized crack opening distribution. Consequently, the corresponding ranges of crack opening for each of stages are represented for the studied soil.

References

1. Albrecht, B. A. and Benson, C. H. (2001), "Effect of Desiccation on Compacted Natural Clays", *Journal of Geotechnical and Geoenvironmental Engineering*, Vol.127, No.1, pp.67-75.
2. Fredlund, D. G. (2006), "Unsaturated Soil Mechanics in Engineering Practice", *Journal of Geotechnical and Geoenvironmental Engineering*, Vol.132, No.3, pp.286-321.
3. Horgan, G. W. and Young, I. M. (2000), "An Empirical Stochastic Model for the Geometry of Two-dimensional Crack Growth in Soil", *Geoderma*, Vol.96, Issue. 4, pp.263-276.
4. Hu, L. B., Peron, H., Hueckel, T. and Laloui, L. (2006), "Numerical and Phenomenological Study of Desiccation of Soil", *Advances in Unsaturated Soil, Seepage, and Environmental Geotechnics (GSP 148)*, Proceedings of Sessions of GeoShanghai 2006, pp.166-173.
5. Jian, Z. and Jian-lin, Y. (2005), "Influences Affecting the Soil-Water Characteristic Curve", *Institute of Geotechnical Engineering*, Vol.6, No.8, pp.797-804.
6. Kamiya, K., Bakrie, R. and Honjo, Y. (2006), "A New Method for the Measurement of Air Permeability Coefficient of Unsaturated Soil", *Proceedings of the Fourth International Conference on Unsaturated Soils*, Vol.2, pp.1741-1752.
7. Kodikara, J. K., Barbour, S. L. and Fredlund, D. G. (1999), "Changes in Clay Structure and Behavior due to Wetting and Drying", *Proceedings of the 8th Australian-New Zealand Conference on Geomechanics, Hobart Tasania*, pp.179-186.
8. Kodikara, J. K., Barbour, S. L. and Fredlund, D. G. (2000), "Desiccation Cracking of Soil Layers", *Unsaturated Soils for Asia*, Rahardjo, Toll & Leong (eds). Balkema, Rotterdam, ISBN 90 5809 139 2, pp.693-698.
9. Konrad, J.-M. and Ayad, R. (1997), "Desiccation of a Sensitive Clay: Field Experimental Observations", *Canadian Geotechnical Journal*, Vol.34, No.6, pp.929-942.
10. Lecocq, N. and Vandewalle, N. (2003), "Dynamics of Crack Opening in a One-dimensional Desiccation Experiment", *Physica A: Statistical Mechanics and Its Applications*, Vol.321, Issues. 3-4, pp.431-441.
11. Liu, C. W., Chen, S. K. and Jang, C. S. (2004), "Modelling Water Infiltration in Cracked Paddy Field Soil", *Hydrological Processes*, Vol.18, No.13, pp.2503-2513.
12. Mal, D., Sinha, S., Mitra, S. and Tarafdar, S. (2005), "Formation of Crack Networks in Drying Laponite Films", *Physica A: Statistical Mechanics and Its Applications*, Vol. 346, Issues. 1-2, pp.110-115.
13. Min, T. K. and Vo-Dai, N. (2007), "A Simple Model of Shrinkage Cracking Development for Kaolinite", *Journal of the Korean Geotechnical Society*, Vol.23, No.9, pp.29-37.
14. Morris, P. H., Graham, J. and Williams, D. J. (1993), "Cracking in Drying Soils", *International Journal of Rock Mechanics and Mining Science & Geomechanics Abstracts*, Vol.30, No.2, pp. 263-277.
15. Peng, X., Horn, R., Peth, S. and Smucker, A. (2006), "Quantification of Soil Shrinkage in 2D by Digital Image Processing of Soil Surface", *Soil & Tillage Research*, Vol.91, Issues. 1-2, pp.173-180.
16. Sharma, R. S., Mohamed, M. H. A. and Lewis, B. A. (2002), "Prediction of Degree of Saturation in Unsaturated Soils Using Image Analysis Technique", *Unsaturated Soils*, The Proceedings of the 3rd International Conference on Unsaturated Soils (UNSAT 2002) Recife, Brazil, Vol.1, pp.369-374.
17. Sharma, R. S. and Mohamed, M. H. A. (2003), "An Experimental Investigation of LNAPL Migration in an Unsaturated/Saturated Sand", *Engineering Geology*, Vol.70, Issues. 3-4, pp.305-313.
18. Sillers, W. S. and Fredlund, D. G. (2002), "Statistical Assessment of Soil-water Characteristic Curve Models for Geotechnical Engineering", *Canadian Geotechnical Journal*, Vol.38, No.6, pp. 1297-1313.
19. Sriboonlue, V., Srisuk, K., Konyai, S. and Khetkratok, N. (2006), "Unsaturated Hydraulic Conductivity for upward Flow in Soil", *Proceedings of the Fourth International Conference on Unsaturated Soils*, Vol.2, pp.1503-1512.
20. Tay, Y. Y., Stewart, D. I. and Cousens, T. W. (2001), "Shrinkage and Desiccation Cracking in Bentonite-Sand Landfill Liners", *Engineering Geology*, Vol.60, Issues. 1-4, pp.263-274.
21. Velde, B. (1999), "Structure of Surface Cracks in Soil and Muds", *Geoderma*, Vol.93, Issues. 1-2, pp.101-124.
22. Velde, B. (2001), "Surface Cracking and Aggregate Formation Observed in a Rendzina Soil, La Touche (Vienne) France", *Geoderma*, Vol.99, Issues. 3-4, pp.261-276.
23. Vogel, H.-J., Hoffmann, H. and Roth, K. (2005), "Studies of Crack Dynamics in Clay Soil I. Experimental Methods, Results, and Morphological Quantification", *Geoderma*, Vol.125, Issues. 3-4, pp. 203-211.
24. Wijeyesekera, D. C. and Papadopoulou, M. C. (2001), "Cracking in Clays with an Image Analysis Perspective", *Clay Science for Engineering*, Adachi & Fukue (eds) Balkema, Rotterdam, ISBN 90 5809 175 9, pp.437-482.
25. Yesiller, N., Miller, C. J., Inci, G. and Yaldo, K. (2000), "Desiccation and Cracking Behavior of Three Compacted Landfill Liner Soils", *Engineering Geology*, Vol.57, Issues. 1-2, pp.105-121.
26. Zhang, L. and Chen, Q. (2005), "Predicting Bimodal Soil-Water Characteristic Curves", *Journal of Geotechnical and Geoenvironmental Engineering*, Vol.131, No.5, pp.666-670.

(received on Jan. 8, 2008, accepted on Aug. 13, 2008)